Electronic Supplementary Information (ESI)

Title: Zinc^{2+} ion inhibits SARS-CoV-2 main protease and viral replication *in vitro*.

Authors: Love Panchariya[a]†, Wajahat Ali Khan[a]†, Shobhan Kuila[a]†, Kirtishila Sonkar[a], Sibasis Sahoo[a], Archita Ghoshal[a], Ankit Kumar[b], Dileep Kumar Verma[b], Abdul Hasan[b], Mohd Azeem Khan[a], Niyati Jain[c], Amit Kumar Mohapatra[d], Shubhashis Das[e], Jitendra K Thakur[e], Souvik Maiti[f], Ranjan Kumar Nanda[d], Rajkumar Halder[g], Sujatha Sunil[b], Arulandu Arockiasamy[a]*

Affiliation:

[a]Membrane Protein Biology Group, International Centre for Genetic Engineering and Biotechnology, Aruna Asaf Ali Marg, New Delhi-110067. India.

[b]Vector Borne Diseases Group, International Centre for Genetic Engineering and Biotechnology, Aruna Asaf Ali Marg, New Delhi-110067. India.

[c]Institute of Genomics and Integrative Biology, CSIR-Institute of Genomics and Integrative Biology, Near Jubilee Hall, Mall Road, Delhi -110007.

[d]Translational Health Group, International Centre for Genetic Engineering and Biotechnology, New Delhi -110067, India.

[e]Plant Mediator Lab, National Institute of Plant Genome Research, Aruna Asaf Ali Marg, New Delhi- 110 067.

[f]CSIR-Institute of Genomics and Integrative Biology, Mathura Road, New Delhi, 110025, India; Academy of Scientific and Innovative Research (AcSIR), Ghaziabad, 201002, India.

[g]Ruhvenile Biomedical OPC PVT LTD, Plot No-8, OCF Pocket Institution, Sarita Vihar, New Delhi-110070. India

†These authors contributed equally to the work presented.

*Correspondence should be addressed to: sam@icgeb.res.in / asamy001@gmail.com

Communicating author:

Arockiasamy Arulandu
International Centre for Genetic Engineering and Biotechnology (ICGEB),
Aruna Asaf Ali Marg,
New Delhi 110067. India.
Phone: +91-11-26741358 Ext-172
Fax: +91-11-26742316
Mobile: +91-9711055502

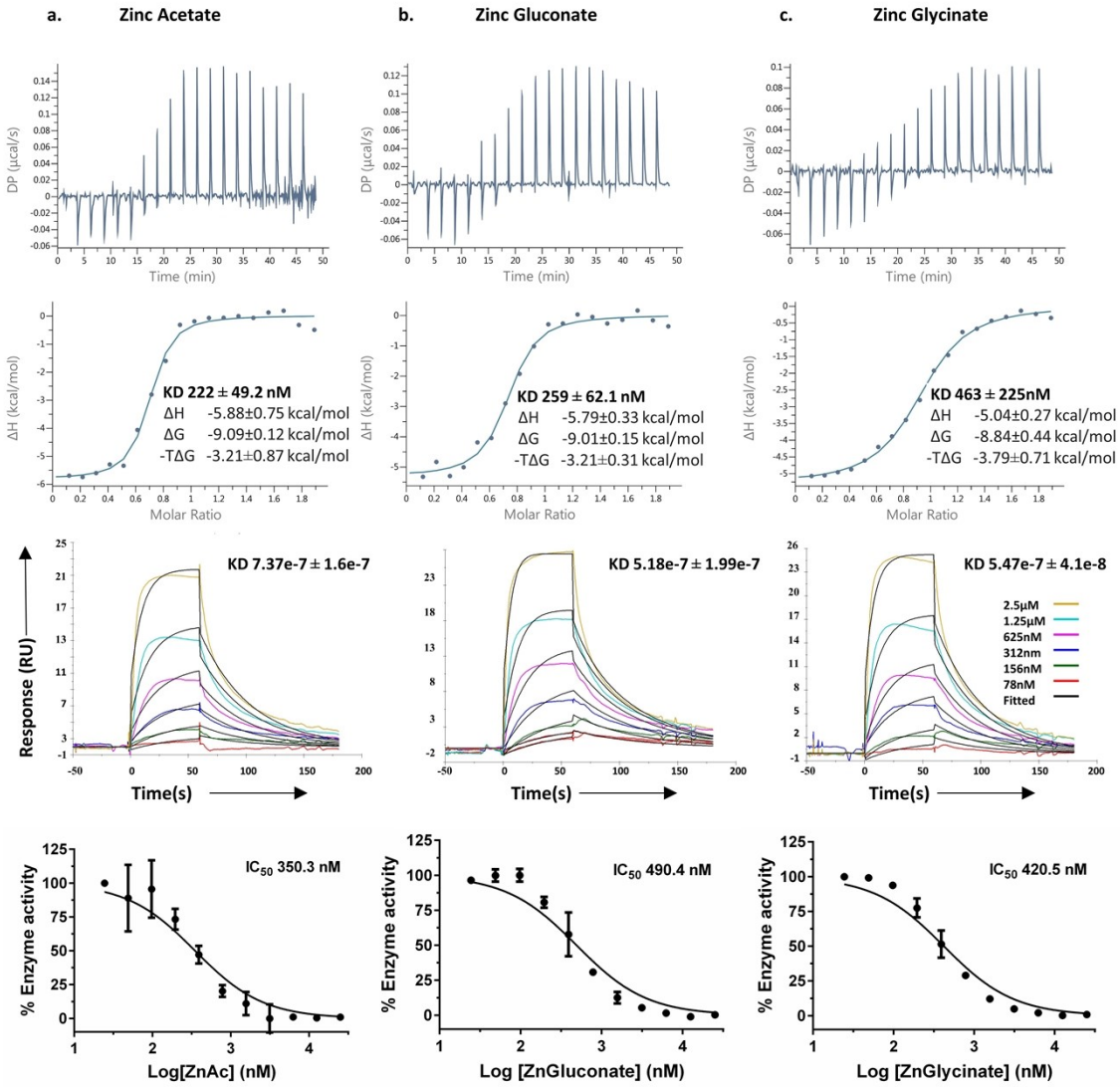

ESI Figure S1. Zn2+ binds and inhibits SARS-COV-2 Mpro. Comparative binding analysis of various Zinc salts with Mpro using ITC and SPR is shown along with concentration dependent inhibition of Mpro enzyme activity by (a) Zinc Acetate (b) Zinc Gluconate (c) Zinc Glycinate.

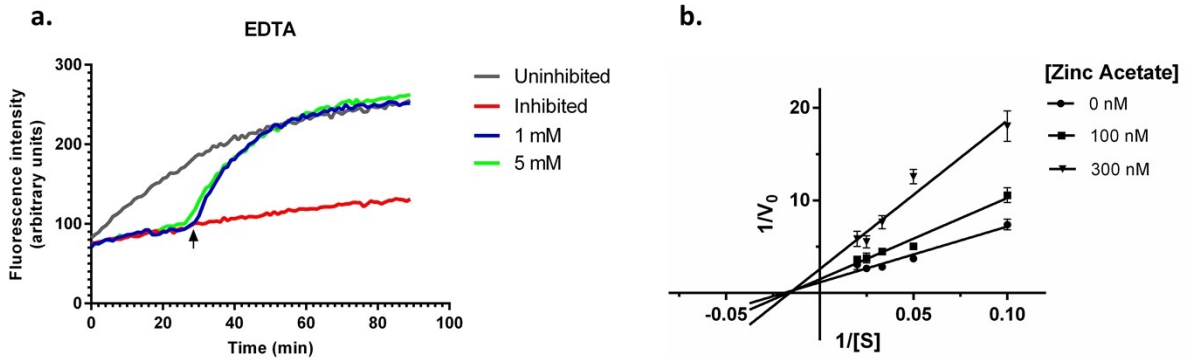

ESI Figure S2. Zinc reversibly binds to SARS-CoV-2 Mpro and inhibits enzyme activity by non-competitive mode of inhibition. (a) Inhibition with 500 nM Zinc acetate was completely reversed by the addition of 1 and 5 mM of EDTA at the 28th minute (represented by an arrow) of the ongoing enzymatic reaction. (b) Lineweaver-burk plot showing non-competitive mode of inhibition of Zn^{2+}.

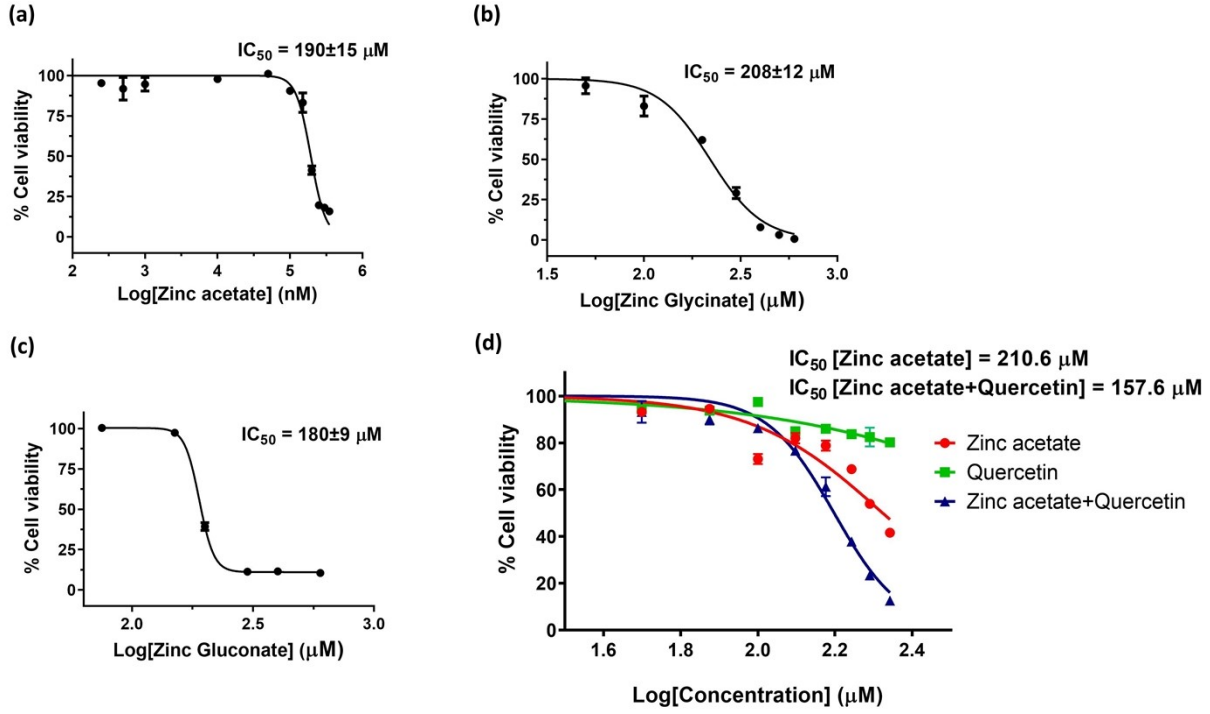

ESI Figure S3. Toxicity determination of Zinc and its complexes in Vero E6 cells. Non-toxic concentrations were determined by studying the effect of Zinc acetate (a), Zinc glycinate (b), and Zinc gluconate (c) on the proliferation of Vero E6 cells after 48 h post addition, as determined by MTT assays. (d) Non-toxic concentrations for Zinc acetate and Quercetin (1:1 molar ratio, blue) is compared with Zinc acetate alone (red). IC_{50} for Quercetin alone (green) could not be determined. Also, IC_{50} for Zinc acetate and Quercetin at 1:2 ratio could not be achieved (not shown). All experiments were done in biological triplicates.

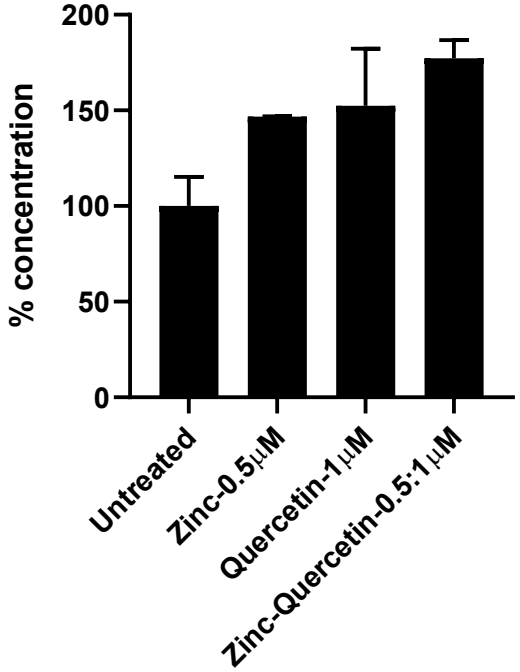

ESI figure S4: ICP-MS quantitation of intracellular Zinc. Zn^{2+} concentration (%) in Vero E6 cells treated with 0.5 μM Zinc acetate, 1 μM Quercetin, and Zinc acetate: Quercetin in a ratio of 0.5:1 μM for 24 h. Bar graph represent data as mean (± SD).

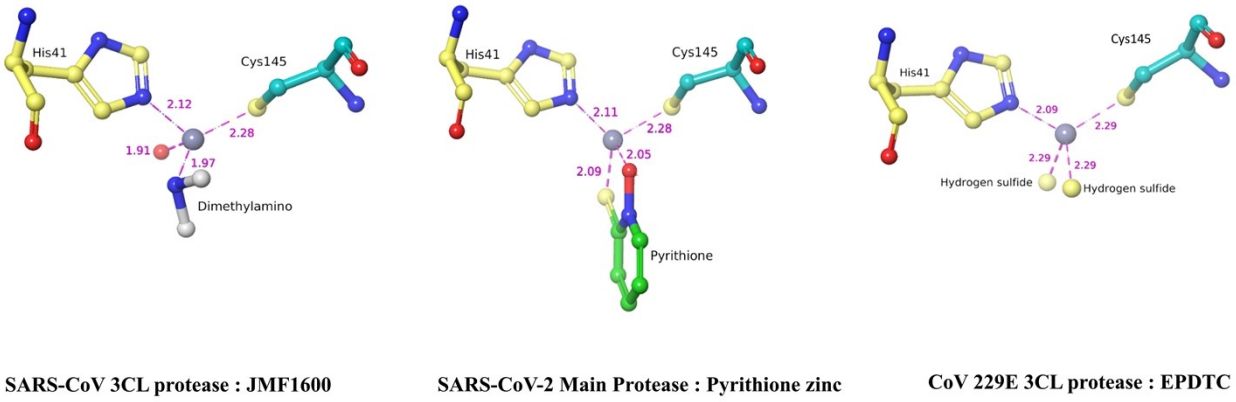

ESI Figure S5: Metal ion coordination of Zinc-complexes bound to coronavirus 3C-like proteases. Ball and stick model representation of 3CL-pro-Zn complex crystal structures; SARS-CoV-Mpro-JMF1600 (PDB: 2Z9K), SARS-CoV-2-Mpro-Zn-pyrithione (PDB: 7B83) and HCoV-229E-3CLpro-N-ethyl-n-phenyl-dithiocarbamic acid (EPDTC) (PDB: 2ZU2). Zinc is depicted as grey ball. Interatomic distances are represented as dotted lines with bond distance in angstrom (Å).

65

	Mpro-Zn^{2+} (PDB:7DK1)	**Mpro-Apo (control)**
Data collection		
Space group	P 2_1 2_1 2_1	P 2_1 2_1 2_1
Cell dimensions		
a, *b*, *c* (Å)	67.6, 102.2, 102.3	67.7, 100.7, 104.0
α, β, γ (°)	90, 90, 90	90, 90, 90
R_{merge}	0.09	0.086
Resolution (Å)	72.32 – 1.90	56.79 – 1.81
$I / \sigma I$	2.69 (1.9)	2.44 (1.8)
Completeness (%)	100.0	100.0
Redundancy	12.8	12.8
Refinement		
Resolution (Å)	72.32 – 1.90	56.79 – 1.81
No. reflections	56,431	66,014
R_{work} / R_{free}	0.191/ 0.213	0.187/0.216
No. atoms		
Protein	4,582	4,649
Ligand/ion	40	38
Water	423	617
B-factors		
Protein	32.4	29.4
Zinc ion	40.75	-
R.m.s. deviations		
Bond lengths (Å)	0.41	0.39
Bond angles (°)	0.58	0.58

66

67 **ESI Table S1. X-ray data processing and refinement statistics**. The data given is for SARS-
68 CoV-2 Apo-Mpro and Mpro-Zn^{2+} complex crystals, both crystallized in the same condition.

69

70 **Materials and methods:**

71 **SARS-CoV-2 Mpro purification**: *E. coli* overexpression plasmid pGEX-6p-1 containing SARS-
72 CoV-2 Mpro was a kind gift from Rolf Hilgenfeld, Institute of Biochemistry, University of
73 Lübeck, Lübeck, Germany [1,2]. The procured construct is designed to generate authentic N terminus
74 by auto-proteolytic cleavage via Mpro at the cleavage-site SAVLQ↓SGFRK (arrow represents the
75 cleavage site). Authentic C-terminus was generated by cleaving the C-terminus 6X His-tag at
76 SGVTFQ↓GP by HRV3C protease. Overexpression and protein purification were performed
77 according to a previous report[2] with some modifications. Expression plasmid was transformed into
78 *E. coli* BL21 (DE3). Transformed cells were inoculated into 200 mL LB media (Luria Bertani
79 Broth, Miller, Himedia) supplemented with ampicillin (100 µg/mL) and grown at 37 °C for 3 h at
80 100 RPM. The primary culture was used to inoculate 6 L of LB media supplemented with
81 ampicillin and induced with 0.5 mM of isopropyl-D-thiogalactoside (IPTG) after OD_{600} reached
82 0.8 at 37 °C. 5 h post induction at 37 °C, cells were harvested by centrifugation at 4000 RPM for
83 20 min at 4 °C and stored at -20 °C until further use. The frozen cell pellet was resuspended in lysis
84 buffer (20 mM Tris, 150 mM NaCl, 10 mM imidazole, 10 µg\ml DNase-I, 100 µg\ml Lysozyme,
85 pH 7.8) and subjected to lysis by sonication on ice, followed by centrifugation at 13000 RPM for
86 50 min at 4 °C. The supernatant was loaded onto serially connected 2x 5ml HisTrap FF columns
87 (GE) at 0.5 ml/min flow rate, pre-equilibrated with buffer A (20 mM Tris, 150 mM NaCl, 10 mM
88 Imidazole pH 7.8). Non-specifically bound proteins were removed by washing with 5 column
89 volumes (CV) of buffer A. The bound proteins were eluted using buffer B (20 mM Tris, 150 mM
90 NaCl, 500 mM imidazole, pH 7.8) with a linear gradient of 10 to 500 mM imidazole. Fractions
91 containing Mpro were pooled and concentration was estimated using OD_{280} [3] . At this stage, many
92 contaminant proteins were observed. To cleave the C-terminal His-tag, HRV3C[4] protease was
93 mixed with SARS-CoV-2 Mpro in 1:5 ratio (mg/mg) and dialysed into buffer C (20 mM Tris, 150
94 mM NaCl, 1 mM DTT, pH 7.8) overnight at 4 °C. This was followed by one more round of dialysis
95 for 6 h in buffer A to remove DTT. Dialysed and tag-cleaved protein was passed through serially
96 connected 2x 5ml HisTrap FF columns. Flow through containing enriched Mpro was collected and
97 buffer exchanged with buffer D (20 mM Tris, 1 mM DTT, pH 8.0) using a HiPrep 26/10 desalting
98 column (GE). Desalted protein was loaded onto 5 ml HiTrap Q HP column (GE) pre-equilibrated
99 with buffer D, and eluted using a linear gradient of 0 to 500 mM NaCl in 20 CV of buffer E (20
100 mM Tris, 1 M NaCl, 1 mM DTT, pH 8.0). Fractions containing pure Mpro were pooled,

101 concentrated and further purified with gel filtration chromatography using pre-equilibrated HiLoad
102 16/600 Superdex 75 pg column with buffer C at a flow rate of 1 ml/min. Purified protein was
103 concentrated to 27.5 mg/ml, aliquoted and flash frozen in liquid nitrogen and stored at -80 °C until
104 further use.

105

106 **Isothermal Calorimetry:** Calorimetric titration studies were carried out at 25 ºC using MicroCal
107 PEAQ-ITC calorimeter (Malvern Panalytical). Each zinc salt (Zinc Acetate, Zinc Gluconate, Zinc
108 Glycinate and Zinc Chloride) was prepared for the titration studies by dissolving it in the binding
109 buffer (10 mM HEPES pH 7.3, 150 mM NaCl) and diluting it to the concentration of 200 µM.
110 Mpro protein sample was prepared at concentration of 20 µM for the titration studies by
111 exchanging it in the same binding buffer as used for the zinc salts, using desalting PD Spin Trap
112 G-25 column (Cytiva). The zinc salt at 200 µM concentration (loaded on instrument syringe) was
113 titrated into 280 µL of 20 µM protein (loaded in the cell) over 19 injections of 2 µl each. The
114 integrated heat data were fit with one-set of binding site using the Microcal PEAQ ITC analysis
115 software. Each zinc salt titration experiment was repeated three times.

116

117 **Surface Plasmon Resonance (SPR):** Experiments were performed using Biacore T200 with
118 control software V2.0 and Evaluation Software V3.1 (GE Life Sciences). All measurements were
119 made at 25 °C. Running buffer consisted of HBS-N pH 7.3 (10 mM HEPES, 150 mM NaCl, pH
120 adjusted with NaOH). Purified Mpro was immobilized onto a CM5 chip using amine coupling
121 method according to manufacturer's protocols with 420 s of surface activation with freshly
122 prepared 1:1 mixture of 1-ethyl-3-(-3-dimethylaminopropyl) carbodiimide hydrochloride (EDC)
123 and N-hydroxysuccinimide (NHS) followed by 420 s contact time for the protein over the activated
124 surface at a flow rate of 10 µl/min. The protein (50 µg/ml) was immobilized onto the chip surface
125 in 10 mM acetate buffer pH 4.0 achieving an RU of ~15500. The remaining activated carboxy
126 methyl groups on the surface were blocked by an injection of 1 M-ethanolamine-HCl pH 8.5 for 7
127 min. An unmodified flow cell surface was used as a reference for each analysis to check for the
128 non-specific binding response to dextran matrix. Running buffer containing varying
129 concentrations of each Zinc salt (Zinc Acetate, Zinc Gluconate, Zinc Glycinate and Zinc Chloride);
130 78 nM to 2.5 µM, were prepared and passed over the immobilized protein at a constant flow rate

131 of 30 μL/min. The interaction (association time 60 s and dissociation time 120 s) between the
132 protein and the analyte resulted in characteristic sensorgrams which were then analysed using
133 Biacore T200 evaluation software; responses generated from unmodified surface were subtracted
134 from the same. The sensorgrams were fitted using 1:1 model to get the association rate [ka (1/Ms)],
135 dissociation rate [kd (1/s)], and equilibrium dissociation constant [KD (M)] for the interaction. The
136 regeneration was done twice using running buffer with 30 s contact time at 50 μL/min flow rate.
137 The experiments were repeated thrice to get the mean values.

138

139 **Mpro enzyme inhibition assay**: Inhibitory roles of Zn^{2+} on enzyme activity were tested via
140 FRET-based enzyme assay[5]. Fluorogenic peptide substrate (Dabcyl)-KTSAVLQ↓SGFRKM-E
141 (Edans)-NH2; (GL Biochem) contains the cleavage site of SARS-COV-2 Mpro (cleavage site
142 represented by ↓). Cleavage of the peptide is marked with an increase in fluorescence from
143 EDANS, which was monitored with microplate reader (Spectramax M3, Molecular devices) at 360
144 nm excitation and 460 nm emission wavelengths.

145 As DTT chelates Zinc ions, SARS-COV-2 Mpro was buffer exchanged into reaction buffer (10
146 mM HEPES pH 7.3, 150 mM NaCl and 0.5 mM TCEP) using PD SpinTrap G-25 column (GE) to
147 remove DTT. 5 μL of Mpro at a final concentration of 200 nM was added to 35 μL pre pipetted
148 reaction buffer in a black 96 well plate. For IC_{50} calculation, 5 μL inhibitor at concentrations
149 ranging from 25 μM to 12.2 nM (2-fold serial dilution), was added to the protein-containing
150 reaction mixture and incubated at 25°C for 30 min with gentle shaking. The reaction was started
151 by adding 5 μL substrate at a final concentration of 20 μM, immediately after which the relative
152 fluorescence was read for 45 min. The total reaction volume was 50 μL. Data were normalized by
153 considering negative control (protein heat inactivated at 60º C for 5 min) as 100% inhibition while
154 treating positive control as 0% inhibition.

155 To test reversibility of Zn^{2+} inhibition, 200 nM protein was first incubated with 500 nM zinc acetate
156 for 30 min at 25º C with gentle shaking as described above. The reaction was then initiated with
157 20 μM substrate. 1 and 5 mM EDTA were added in separate wells at 28th minute when the reading
158 was being taken.

159

160 **SARS-CoV-2 Mpro crystallization and soaking with Zinc:** Purified protein was diluted to 13.6
161 mg/ml for crystallization in buffer C. Several flower-like multi-crystals were obtained after
162 overnight incubation at 20º C in the reservoir solution containing 100 mM Bis-Tris, 20% PEG
163 3350 and 5% DMSO pH 6.5[6]. These multi-crystals were used to prepare seeds using seed beads
164 (Hampton research). Seeding was done into 3 µL protein: reservoir (2:1) drop in a 24 well sitting
165 drop plate (Hampton research). Thereafter, single crystals with thin plate-like morphology were
166 obtained after overnight incubation. Reservoir containing 10 mM Zinc glycinate or Zinc gluconate
167 (TCI chemicals #G0215 and #G0277, respectively) was added to wells containing good quality
168 crystals and soaked for 4 h. Crystals were then fished out and cryo-protected in a solution
169 containing the reservoir with 20% glycerol. Subsequently, crystals were immediately flash-frozen
170 into liquid nitrogen and stored for further X-ray diffraction and data collection. Multiple attempts
171 to co-crystallize with zinc salts failed due to heavy precipitation of the protein. Also, soaking
172 solutions containing Zn^{2+} such as Zinc acetate or Zinc sulphate deteriorated the crystal quality.

173

174 **X-ray data collection, processing and refinement:** X-ray diffraction data for Zinc-soaked
175 SARS-CoV-2 Mpro crystals were collected at XRD2 beamline[7], Elettra Sincrotrone Trieste at
176 0.99Å wavelength on a Dectris Pilatus 6M detector. Collected data were processed with
177 autoPROC[8] and structure was determined by molecular replacement using Phaser-MR of Phenix
178 crystallographic suite[9] using 6Y2F as search template. Initial model building was done with
179 AutoBuild[10] module. Structure and map quality were further improved by manual building with
180 Coot[11] and refinement with autoBUSTER[12]. Refinement statistics are summarised in
181 Supplementary Table 2. Final model has R_{work} and R_{free} of 0.19 and 0.21 respectively. The structure
182 has no Ramachandran outliers and 0.8 % side chain outliers. Figures were made with UCSF
183 Chimera[13] and Maestro, Schrodinger suite (Licenced to ICGEB).

184

185 **Molecular Dynamics:** Crystal structure of SARS-CoV-2 Mpro with Zinc (PDB: 7DK1) was
186 prepared with protein preparation wizard of Schrodinger suite. Protonation states at pH 7.4±0.5
187 were created for the complex, explicit hydrogens were added to the structure, and zero bond order
188 was created for Zn^{2+} ion. Hydrogen bond optimization was done with ProtAssign and finally

189 restrained minimization was performed using OPLS3e force field to obtain input structure for
190 further calculations and analysis before performing Molecular Dynamic (MD) simulations.

191 To analyse the stability of the SARS-CoV-2 Mpro-Zinc complex, a 1 μs MD simulation was
192 performed using Desmond[14] (Schrodinger) and the coordinates were saved at an interval of 50 ps.
193 Simulation system was built using OPLS3e force field and solvated with TIP3P water model.
194 Orthorhombic box with an edge length of 10 Å was set, ensuring a minimal distance between the
195 atoms of protein complex and edge of the box. Counter ions were added to neutralize the system;
196 further, 0.15 M NaCl was added to the solvated box as salt. The prepared systems were relaxed
197 before the actual simulation by a series of energy minimization and short MD simulations, which
198 mainly comprise of six relaxation steps while keeping the solute restrained. Briefly, in the first two
199 steps, systems were relaxed with Brownian Dynamics NVT at T=10 K for 100 ps and 12 ps
200 respectively. In step 3 and 4, NPT equilibration was done for 12 ps at 10 K with restrains on heavy
201 solute atoms. At step 5, the pocket was solvated. Finally, in step 6 and 7 short NPT equilibrations
202 were done for 12 and 24 ps respectively. The NPT ensemble was employed for the simulations
203 with Nose-Hover chain thermostat and the Maryna-Tobias-Klein barostat. RESPA integrate was
204 used with a time step of 2 fs. For short range of coulombic interactions, a 9 Å cut off was
205 considered. Analysis of the simulation was done with simulation event analysis, Desmond.

206

207 **Cell culture and virus strain**: Vero E6 cells (African green monkey kidney cells) were purchased
208 from ATCC, grown and maintained in Minimal Essential Media (MEM; HIMEDIA; AL047S)
209 supplemented with 10 % FBS (HIMEDIA, RM10681), 2 mM L-Glutamine (HIMEDIA; TCL012),
210 100 U/ml penicillin, and 10 mg/ml streptomycin, in a 5 % carbon dioxide incubator with controlled
211 humidity at 37 °C. For antiviral studies, SARS-CoV-2 strain, USA-WA1/2020 was used. All the
212 virus infection and subsequent experiments using virus were performed in BSL-3 (virology)
213 facility at ICGEB, New Delhi.

214

215 **Cell viability assay:** Cytotoxicity of Zinc acetate, Zinc glycinate, and Zinc gluconate on the
216 viability and proliferation of the Vero E6 cells was evaluated using MTT assay. Cells were seeded
217 at a density of 7000 cells per well in a 96-well plate. After allowing the cells to attach overnight,
218 they were treated with varying concentrations of the above compounds. Treatment was done in

219 MEM supplemented with 2% FBS for 48 h, at the end of which MTT assay was performed as per
220 manufacturer's protocol. GraphPad Prism software was used to determine the IC_{50} (50% inhibitory
221 concentration). The absorbance (A) was measured at 570 nm and the percentage cell viability was
222 calculated using the following formula:
223 Percentage cell viability = (A_{570} of treated)/A_{570} of Untreated) *100
224
225 **Zn quantification using inductively coupled plasma-mass-spectrometry (ICP-MS):** Briefly,
226 Vero E6 cells after incubating with Zinc acetate (0.5 µM), Quercetin (1 µM), and Zinc acetate:
227 Quercetin (0.5 µM:1 µM) for 24 h were harvested by trypsinization. After washing with PBS, cells
228 were passed through a treated Chelex-100 resin (#C7901, Sigma) column. The harvested cells
229 were counted before centrifuging and the cell pellets were digested in HNO_3 (70%, #425711,
230 Sigma Aldrich) overnight at room temperature. The acid digestion was stopped using H_2O_2 (30%,
231 #1.07298.1000, Supelco) and further diluted in trace metal free water (#95305, Honeywell
232 TraceSELECT) before quantifying Zn (m/z:65.9260) levels using iCAP™ TQ ICP-MS (Thermo
233 Scientific, USA). The diluted samples were taken up by the ICP-MS by self-aspiration using a
234 sample capillary (0.55 mm) to a nebulizer and spray chamber. Using a multi elemental standard
235 mix (#92091, Sigma Aldrich), a calibration curve from 1 part per billion (ppb) to 1 part per million
236 (ppm) was drawn (R^2= 0.99) and used for absolute quantification of Zn levels in test samples.
237
238 **Anti-SARS-CoV-2 assay:** Anti-viral assays with Zinc acetate, Zinc gluconate and Zinc glycinate
239 were performed using a standard assay reported for SARS-CoV-2 and other viruses[15,16]. Vero E6
240 cells were seeded in 24-well plates, a day prior to infection. The following day, Zinc and other
241 compounds were added to these seeded cells at maximum non-toxic concentration (100 µM, 70
242 µM and 100 µM respectively) followed by infection with SARS-COV-2 (Multiplicity of infection;
243 MOI= 0.1). The treated and virus infected cells were incubated for 48 h (37 °C, 5% CO_2) following
244 which the supernatants were harvested for viral quantification by plaque assay and qRT-PCR. 2%
245 FBS in MEM media was used in anti-SARS-CoV-2 assays following the already published
246 protocol[17].
247
248 **Plaque assay:** For viral quantification, Vero E6 cells were seeded in 96 well plates, followed by
249 viral inoculation on the next day using dilutions; starting at 1:50 the virus was double diluted till

250 1:51200. The virus was incubated with the cells for 2 h at 37 °C for viral adsorption. Thereafter,
251 the media containing the inoculum was removed, and wells were overlaid with 150 µL of 1%
252 carboxymethylcellulose (CMC) prepared in MEM media (containing 5% FBS). In plaque assay
253 2% FBS was used for inoculation step. The plates were then incubated at 37 °C for 96 h with 5%
254 CO_2 and 75% humidity. Post incubation, the cells were fixed with 5% formaldehyde before
255 washing twice with 1× PBS and staining was performed using 0.25% crystal violet (prepared in
256 30% methanol). Plaques were visualized and counted to calculate viral titers using the following
257 formula: Plaque forming units (pfu) = (No. of plaques)/ (Dilution × volume of virus).
258
259 **qRT-PCR:** To quantify the viral RNA using qRT-PCR, 150 µL media from the treated, untreated
260 and virus infected wells was collected, and used for RNA isolation using the NucleoSpin Viral
261 RNA isolation kit (740956.250). Isolated RNA samples were then subjected to One-step qRT-PCR
262 using QuantiTect qRT-PCR kit (Qiagen #1054498) and PIKOREAL 96 Real-Time PCR system
263 (Thermo scientific). Data analysis was performed using a standard curve to calculate genome
264 equivalents of SARS-CoV-2 in all the samples.
265
266 **References:**

267 1. F. Wu, S. Zhao, B. Yu, Y. M. Chen, W. Wang, Z. G. Song, Y. Hu, Z. W. Tao, J. H. Tian,
268 Y. Y. Pei, M. L. Yuan, Y. L. Zhang, F. H. Dai, Y. Liu, Q. M. Wang, J. J. Zheng, L. Xu,
269 E. C. Holmes and Y. Z. Zhang, *Nature*, 2020, **579**, 265-269.
270 2. R. Hilgenfeld, *FEBS Journal*, 2014, **281**, 4085-4096.
271 3. C. N. Pace, F. Vajdos, L. Fee, G. Grimsley and T. Gray, *Protein Sci*, 1995, **4**, 2411-2423.
272 4. S. Raran-Kurussi and D. S. Waugh, *Anal Biochem*, 2016, **504**, 30-37.
273 5. R. Y. Kao, A. P. To, L. W. Ng, W. H. Tsui, T. S. Lee, H. W. Tsoi and K. Y. Yuen, *FEBS*
274 *Lett*, 2004, **576**, 325-330.
275 6. D. W. Kneller, G. Phillips, H. M. O'Neill, R. Jedrzejczak, L. Stols, P. Langan, A.
276 Joachimiak, L. Coates and A. Kovalevsky, *Nat Commun*, 2020, **11**, 3202.
277 7. A. Lausi, M. Polentarutti, S. Onesti, J. R. Plaisier, E. Busetto, G. Bais, L. Barba, A.
278 Cassetta, G. Campi, D. Lamba, A. Pifferi, S. C. Mande, D. D. Sarma, S. M. Sharma and
279 G. Paolucci, *The European Physical Journal Plus*, 2015, **130**, 43.
280 8. C. Vonrhein, C. Flensburg, P. Keller, A. Sharff, O. Smart, W. Paciorek, T. Womack and
281 G. Bricogne, *Acta Crystallogr D Biol Crystallogr*, 2011, **67**, 293-302.
282 9. D. Liebschner, P. V. Afonine, M. L. Baker, G. Bunkoczi, V. B. Chen, T. I. Croll, B.
283 Hintze, L. W. Hung, S. Jain, A. J. McCoy, N. W. Moriarty, R. D. Oeffner, B. K. Poon,
284 M. G. Prisant, R. J. Read, J. S. Richardson, D. C. Richardson, M. D. Sammito, O. V.
285 Sobolev, D. H. Stockwell, T. C. Terwilliger, A. G. Urzhumtsev, L. L. Videau, C. J.
286 Williams and P. D. Adams, *Acta Crystallogr D Struct Biol*, 2019, **75**, 861-877.

287 10. T. C. Terwilliger, R. W. Grosse-Kunstleve, P. V. Afonine, N. W. Moriarty, P. H. Zwart,
288 L. W. Hung, R. J. Read and P. D. Adams, *Acta Crystallogr D Biol Crystallogr*, 2008, **64**,
289 61-69.
290 11. P. Emsley, B. Lohkamp, W. G. Scott and K. Cowtan, *Acta Crystallogr D Biol*
291 *Crystallogr*, 2010, **66**, 486-501.
292 12. B. E. Bricogne G., Brandl M., Flensburg C., Keller P., Paciorek W., and S. A. Roversi P,
293 Smart O.S., Vonrhein C., Womack T.O, *Journal*, 2017.
294 13. E. F. Pettersen, T. D. Goddard, C. C. Huang, G. S. Couch, D. M. Greenblatt, E. C. Meng
295 and T. E. Ferrin, *J Comput Chem*, 2004, **25**, 1605-1612.
296 14. J. C. Phillips, R. Braun, W. Wang, J. Gumbart, E. Tajkhorshid, E. Villa, C. Chipot, R. D.
297 Skeel, L. Kale and K. Schulten, *J Comput Chem*, 2005, **26**, 1781-1802.
298 15. L. Caly, J. D. Druce, M. G. Catton, D. A. Jans and K. M. Wagstaff, *Antiviral Res*, 2020,
299 **178**, 104787.
300 16. P. Kalita, A. K. Padhi, K. Y. J. Zhang and T. Tripathi, *Microb Pathog*, 2020, **145**,
301 104236.
302 17. A. J. te Velthuis, S. H. van den Worm, A. C. Sims, R. S. Baric, E. J. Snijder and M. J.
303 van Hemert, *PLoS Pathog*, 2010, **6**, e1001176.

304